JACS
JOURNAL OF THE AMERICAN CHEMICAL SOCIETY
Article
pubs.acs.org/JACS

Synthesis and Arm Dissociation in Molecular Stars with a Spoked Wheel Core and Bottlebrush Arms

Joanna Burdyńska,[†] Yuanchao Li,[‡] Anant Vikas Aggarwal,[§] Sigurd Höger,*[,§] Sergei S. Sheiko,*[,‡] and Krzysztof Matyjaszewski*[,†]

[†]Center for Macromolecular Engineering, Department of Chemistry, Carnegie Mellon University, 4400 Fifth Avenue, Pittsburgh, Pennsylvania 15213, United States

[‡]Department of Chemistry, University of North Carolina at Chapel Hill, Chapel Hill, North Carolina 27599-3290, United States

[§]Kekulé-Institut für Organische Chemie und Biochemie, Rheinische Friedrich-Wilhelms-Universität Bonn, Gerhard-Domagk-Straße 1, 53121 Bonn, Germany

Supporting Information

ABSTRACT: Unique star-like polymeric architectures composed of bottlebrush arms and a molecular spoked wheel (MSW) core were prepared by atom transfer radical polymerization (ATRP). A hexahydroxy-functionalized MSW ($\mathbf{MSW_{6\text{-}OH}}$) was synthesized and converted into a six-fold ATRP initiator ($\mathbf{MSW_{6\text{-}Br}}$). Linear chain arms were grafted from $\mathbf{MSW_{6\text{-}Br}}$ and subsequently functionalized with ATRP moieties to form six-arm macroinitiators. Grafting of side chains from the macroinitiators yielded four different star-shaped bottlebrushes with varying lengths of arms and side chains, i.e., $\mathbf{(450\text{-}\textit{g}\text{-}20)_6}$, $\mathbf{(450\text{-}\textit{g}\text{-}40)_6}$, $\mathbf{(300\text{-}\textit{g}\text{-}60)_6}$, and $\mathbf{(300\text{-}\textit{g}\text{-}150)_6}$. Gel permeation chromatography analysis and molecular imaging by atomic force microscopy confirmed the formation of well-defined macromolecules with narrow molecular weight distributions. Upon adsorption to an aqueous substrate, the bottlebrush arms underwent prompt dissociation from the MSW core, followed by scission of covalent bonds in the bottlebrush backbones. The preferential cleavage of the arms is attributed to strong steric repulsion between bottlebrushes at the MSW branching center. Star-shaped macroinitiators may undergo aggregation which can be prevented by sonication.

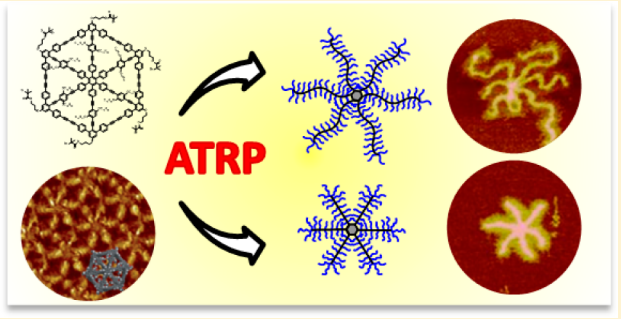

INTRODUCTION

Continuous development in the areas of controlled radical polymerization (CRP) and organic synthesis has given researchers access to a variety of complex macromolecules with a vast number of well-defined topologies.[1−3] In particular, molecular bottlebrushes, a unique type of graft copolymers with side chains densely packed along a linear polymer chain, have garnered a great deal of attention.[4−11] The high grafting density generates strong steric repulsion between the tethered side chains, resulting in the corresponding increase in the persistence length and disentanglement of bottlebrushes. A distinct worm-like conformation of molecular bottlebrushes, along with their exceptional length[12] (up to several micrometers), affords the ability to image individual molecules using atomic force microscopy (AFM). Therefore, molecular bottlebrushes have been widely used as model systems for experimental studies of single-molecule ordering, motion, and reactivity at interfaces.[8]

In synthetic chemistry, dense grafting has been explored as a versatile platform for the design of complex molecular and supramolecular systems with bottlebrushes as shape-persistent mesoblocks. Bottlebrushes can be prepared via three different approaches: "grafting through",[13] "grafting onto",[14] and "grafting from".[4,8,15−17] CRP techniques, in particular atom transfer radical (ATRP),[3,18−20] reversible addition−fragmentation chain transfer (RAFT,)[21,22] and nitroxide-mediated polymerizations (NMP),[23] have provided a convenient route for the preparation of well-defined molecular brushes. Both the grafts and backbones may have different branching topologies and chemical compositions that can be altered separately, which exceedingly expands the range and sophistication of molecular architectures, and thus materials' properties as compared to those of linear polymers. Up to now, a variety of densely grafted copolymers with different architectures were prepared including brush-coil,[24] diblock (both within the backbone and side chains),[21,25−30] gradient,[31,32] and multi-arm star-like brushes.[33] Such unique macromolecules have also been extensively investigated in areas of supersoft elastomers,[34,35] photonics,[10,28,29,36] organic nanotubes,[11,21] biomimetic materials,[37−39] networks and porous materials,[27,40] and lithography/nanofabrication.[41,42]

Received: July 8, 2014
Published: August 18, 2014

   dx.doi.org/10.1021/ja506780y | J. Am. Chem. Soc. 2014, 136, 12762−12770

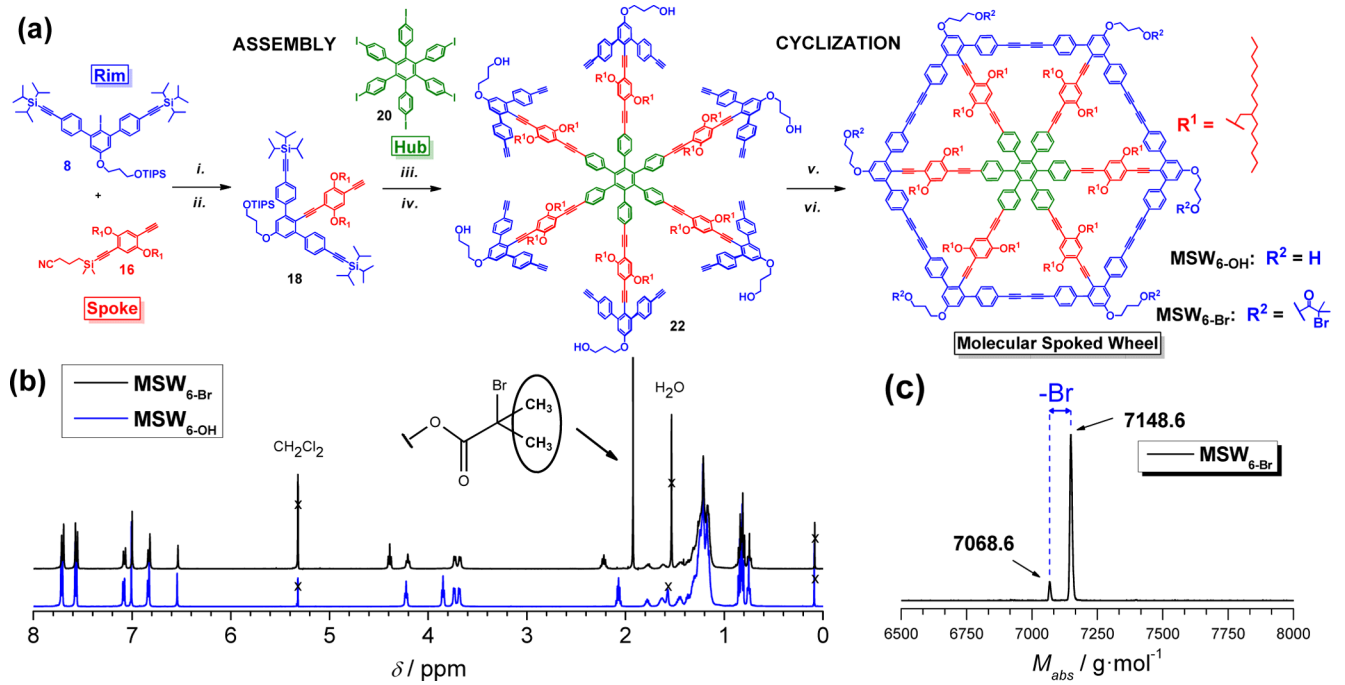

Figure 1. (a) Synthetic approach used for the preparation of molecular spoked wheels (MSWs) and chemical structures of the rim (blue), spoke (red), hub (green), and MSW derivatives. Reagents and conditions: *i*, $Pd(PPh_3)_2Cl_2$, CuI, PPh_3, THF, piperidine, μw (microwave irradiation), 120 °C, 12 min, 92%; *ii*, K_2CO_3, THF, methanol, rt, 2 h, 100%; *iii*, Pd_2dba_3, CuI, dppf, THF, piperidine, 80 °C, 17 h, 81%; *iv*, TBAF, THF, 0 °C to rt, 3 h, 74%; *v*, 2-bromo-2-methylpropionyl bromide, pyridine, CH_2Cl_2, 0 °C, 2 h. (b) NMR spectra of **MSW$_{6\text{-OH}}$** and **MSW$_{6\text{-Br}}$** in CD_2Cl_2. The spectra are very similar, but the methyl groups on the 2-bromo-2-methylpropanoate unit **MSW$_{6\text{-Br}}$** give rise to a new sharp singlet signal at 1.92 ppm. (c) MALDI-TOF of **MSW$_{6\text{-Br}}$** showing the high purity of the 6-fold initiator.

The ATRP initiator can also be designed to modify the architecture of densely grafted copolymers. Previously, the multifunctional ATRP initiators were used to prepare three- and four-armed architectures, which combined the properties of both polymeric stars and molecular bottlebrushes.[33] AFM imaging of individual molecules provided a visual confirmation of star-shaped bottlebrushes, also allowing for the correlation of the type of a catalytic system with the structural quality of obtained polymers. Star-like bottlebrushes displayed a distinct ordering of monolayers, showing transition under compression, from a dendritic to a disk-like conformation.[43]

In this work, we have designed a novel type of molecular spoked wheel (MSW) ATRP initiator, which allows for the synthesis of molecular star bottlebrushes with a higher number of arms than reported previously, and a planar topology that is forced by the disk-like structure of the initiator. MSWs form a new class of conjugated macrocycles with multiple aromatic rings and alkyne groups covalently linked together[44−48] to form exceptionally rigid and highly fluorescent structures.[49−53] These unique molecules can be potentially utilized as optically active materials,[54] molecular wires,[55] or environmentally confined reaction containers.[56] It was also shown previously that they are useful tools for fundamental studies of the understanding of the microscopic electronic structure of conjugated polymers.[50] For the purpose of this study, we have synthesized a six-fold, hydroxy-functionalized MSW (**MSW$_{6\text{-OH}}$**) and converted it to a well-defined ATRP initiator (**MSW$_{6\text{-Br}}$**). The ATRP functionalized MSW allowed for the preparation of star-like bottlebrushes with a distinct hexa-arm topology. Star-shaped bottlebrushes with varying lengths of arms and side chains were generated by grafting poly(*n*-butyl acrylate) from star-like backbones under normal ATRP conditions. Polymers were characterized by gel permeation chromatography (GPC) and AFM, proving the formation of star-shaped polymers. AFM analysis allowed for the direct visualization of star-shaped bottlebrushes with distinctive topological differences resulting from varied lengths of both grafts and arms.

The goal of this work was to synthesize new star-like bottlebrush architectures from a radial, six-fold MSW initiator. We expected to enhance mechanical tension on the MSW through the incorporation of bottlebrush arms, thus causing a distortion of the highly conjugated core. A buildup of steric repulsion at the MSW core led to prompt dissociation of bottlebrush arms, which was observed and studied by AFM. However, no significant changes in electronic properties were detected, as indicated by emission experiments (see SI, Figures S6−S8).[57]

RESULTS AND DISCUSSION

Synthesis and Characterization of the Molecular Spoked Wheel-Based Six-Fold ATRP-Initiator MSW$_{6\text{-Br}}$. The synthetic approach used for the preparation of six-fold **MSW$_{6\text{-Br}}$** ATRP initiator was based on the previous reports on analogous MSWs.[50,58] In this paper, we introduced synthetic adjustments that allowed for the synthesis of **MSW$_{6\text{-Br}}$**. A complete description of synthetic procedures including all organic precursors and sample characterization is given in the Supporting Information (SI).

The synthesis of **MSW$_{6\text{-Br}}$** relied on the preparation of its hexa-hydroxy precursor, **MSW$_{6\text{-OH}}$**. The incorporated hydroxyl functionalities allow post-cyclization modification of the MSW providing access to new, more complex MSWs which can be potentially used in the generation of novel advanced materials. Furthermore, due to the strong propensity of previously

dx.doi.org/10.1021/ja506780y | J. Am. Chem. Soc. 2014, 136, 12762−12770

Scheme 1. Synthesis of Star-like Bottlebrushes with Hexa-arm ATRP Initiator $MSW_{6\text{-}Br}$ via Double "Grafting-from" Approach

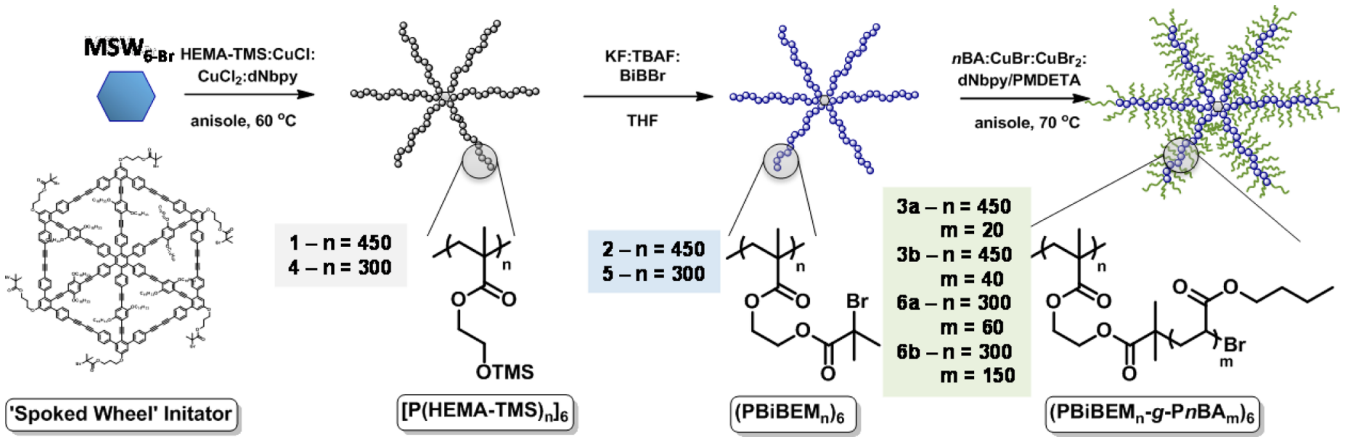

prepared MSWs analogues toward the aggregation, we also aimed to eliminate such tendency in $MSW_{6\text{-}Br}$, thus ensuring the polymerization exclusively from unimolecular initiator species.[58] This was accomplished through the replacement of linear hexadecyl side chains of the spoke, with branched 2-hexyldecyl groups (Figure 1a). As proved by dynamic light scattering (DLS) measurements in chloroform and toluene (Figure S5), the incorporation of the branching in MSWs resulted in the successful suppression of their aggregation. It was ascribed to the reduced ability of MSWs to interact via $\pi-\pi$ stacking as well as their improved solubility as compared to structures with linear hexadecyl groups.

$MSW_{6\text{-}OH}$ was obtained via a convex modular approach, based on the design of individual modules: the **rim** (blue), **spoke** (red) and **hub** (green). All the building blocks were linked together prior the cyclization (Figure 1a). The most crucial step was the design of the functional **rim** (Figure 1a, blue; Figure S2, 8) with incorporated hydroxyl functionality. The structure of the **rim** was based on *m*-terphenyl-scaffold modified with 3-[(triisopropylsilyl)oxy]propyl linker (TIPSO−), which allowed for the incorporation of a protected hydroxyl group into the molecule (Figure 1a; Figure S2, 8). Next, the **rim** was attached to the **spoke** (Figure 1a, red; Figure S2, 16) to form a spoke-rim module (Figure 1a, Figure S2, 18), which was then selectively deprotected and linked to the **hub** (Figure 1a, green; Figure S2, 20). A subsequent deprotection of the assembled product yielded a MSW precursor with six free hydroxyl (Figure 1a, Figure S2, 22) groups, which was directly cyclized under pseudo high-dilution conditions to form the desired $MSW_{6\text{-}OH}$ (Figure 1a). Then, $MSW_{6\text{-}OH}$ was converted into a well-defined ATRP initiator, $MSW_{6\text{-}Br}$ through a six-fold esterification reaction with α-bromoisobutyryl bromide and pyridine (Figure 1a). The esterification of $MWS_{6\text{-}OH}$ proceeded with high yields (89%) and efficiency, as confirmed by the appearance of the signal at 1.94 ppm corresponding to CH_3- protons of ATRP moieties in the ^{1}H NMR spectra of $MSW_{6\text{-}Br}$ (Figure 1b). MALDI-TOF analysis of $MWS_{6\text{-}Br}$ showed the presence of two peaks corresponding to pure molecules and molecules that lost one bromine atom upon ionization (molecular mass 7148.6 and 7068.6 Da, respectively), thus confirming a very high purity of the final ATRP hexa-initiator.

Synthesis and Characterization of $(PBiBEM_{300/450})_6$ Hexa-arm Macroinitiators. The synthetic pathway for the synthesis of star-shaped brushes is shown in Scheme 1. Molecular bottlebrush arms were prepared via double "grafting-from" approach under normal ATRP conditions. First, (2-trimethylsiloxyethyl) methacrylate (HEMA-TMS) was polymerized from the multifunctional ATRP initiator ($MSW_{6\text{-}Br}$), followed by a subsequent esterification with ATRP-active moieties. Finally, poly(*n*-butyl acrylate) side chains were grafted from six-arm ATRP macroinitiators, resulting in star-shaped molecular bottlebrushes (Scheme 1).[33] P(HEMA-TMS) was grafted from $MSW_{6\text{-}Br}$ under normal ATRP conditions to form arms of stars with degrees of polymerization (DPs) of 450 ($(\mathbf{450\text{-}TMS})_6$) and 300 ($(\mathbf{300\text{-}TMS})_6$). Reactions were performed with high molar ratios of [M]:[I] (9600 and 6000 respectively) while keeping polymerizations at limited monomer conversions (~30%), thereby suppressing the intermolecular termination between growing arms, and subsequent star−star coupling. To ensure high initiation efficiencies from the multifunctional initiator, $MSW_{6\text{-}Br}$, the polymerizations of HEMA-TMS were performed with Cu^ICl/dNbpy complex as a catalytic system.[33,59] Earlier results revealed that ATRP reactions under halogen exchange conditions produce well-defined stars with narrow arm length distributions and improved grafting efficiency, as compared to traditionally used Cu^IBr-based catalyst.[33] $[P(HEMA\text{-}TMS)_{450}]_6$ ($(\mathbf{450\text{-}TMS})_6$) and $P(HEMA\text{-}TMS)_{300}]_6$ ($(\mathbf{300\text{-}TMS})_6$) were characterized by GPC confirming the formation of star-polymers (Figure 2, black) with narrow molecular weight distributions (MWDs), M_w/M_n = 1.22 and 1.12, respectively (Table 1, samples **1** and **4**). The number-average molecular weights (M_n) for the macroinitiators $(\mathbf{450\text{-}TMS})_6$ and $(\mathbf{300\text{-}TMS})_6$ were lower than the corresponding theoretical values ($M_{n,th}$). This was attributed to a compact structure of star-shaped P(HEMA-TMS) polymers, which resulted in hydrodynamic volumes smaller than the dimensions of linear poly(methyl methacrylate) (PMMA) standards.

The functionalization of $(\mathbf{450\text{-}TMS})_6$ and $(\mathbf{300\text{-}TMS})_6$ with ATRP reactive groups was performed via one pot, two-step process, following a previously reported procedure.[4] First, TMS-blocked hydroxyl groups were deprotected in the presence of KF/TBAF, followed by the subsequent addition of α-bromoisobutyryl bromide, resulting in the formation of respective PBiBEM macroinitiators $(\mathbf{450\text{-}Br})_6$ and $(\mathbf{300\text{-}Br})_6$. ^{1}H NMR spectroscopy of polymers confirmed the full deprotection of OTMS together with the quantitative incorporation of ATRP functionalities, as indicated by the disappearance of TMS signals and the downfield shift of both adjacent CH_2 peaks of P(HEMA-TMS).[60] GPC character-

dx.doi.org/10.1021/ja506780y | J. Am. Chem. Soc. 2014, 136, 12762−12770

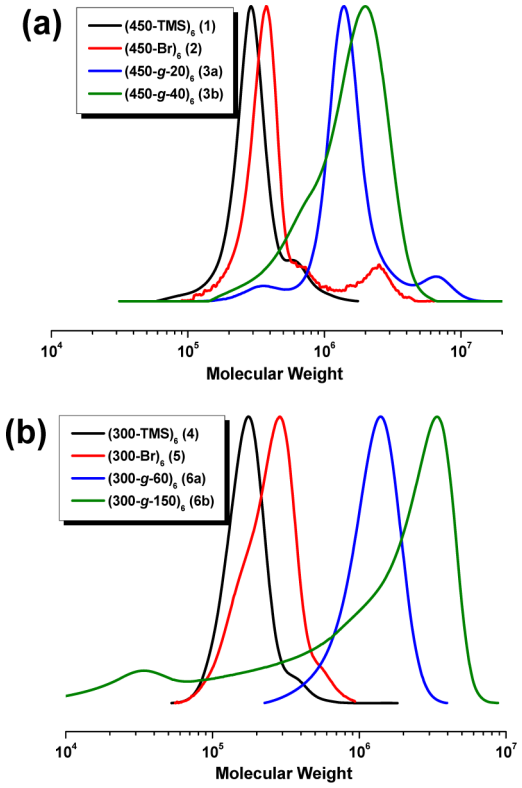

Figure 2. GPC traces of (a) $[P(HEMA\text{-}TMS_{450})]_6$ ((**450-TMS**)$_6$, black), $(PBiBEM_{450})_6$ ((**450-Br**)$_6$, red), $(PBiBEM_{450}\text{-}g\text{-}(PnBA_{20})_6$ ((**450-*g*-20**)$_6$, blue), and $(PBiBEM_{450}\text{-}g\text{-}(PnBA_{40})_6$ ((**450-*g*-40**)$_6$, green); (b) $[P(HEMA\text{-}TMS3_{00})]_6$ ((**300-TMS**)$_6$, black), $(PBiBEM_{300})_6$ ((**300-Br**)$_6$, red), $(PBiBEM_{300}\text{-}g\text{-}(PnBA_{60})_6$ ((**300-*g*- 60**)$_6$, blue), and $(PBiBEM_{300}\text{-}g\text{-}(PnBA_{150})_6$ ((**300-*g*-150**)$_6$, green).

ization of (**450-Br**)$_6$ and (**300-Br**)$_6$ gave respective M_w/M_n = 1.39 and 1.20 (Table 1, samples **2** and **5**), showing no significant shift of signals as compared to the corresponding P(HEMA-TMS) materials (Figure 2, red). Broadening of the MWD of (**450-Br**)$_6$ (Table 1, sample **2**) was related to the presence of a high molecular weight signal in the GPC trace (Figure 2a, red), which was ascribed to a small fraction of polymeric aggregates present in the sample.

During the preparation of (**450-Br**)$_6$, it was noticed that the macroinitiator could undergo aggregation in THF (Figure S9 and S10). However, the process could be readily prevented through sonication of the solution, thus allowing for a full recovery of single (**450-Br**)$_6$ species (Figure S9). We did not observe any measurable backbone scission during sonication at different durations. As shown in Figure S9, sonication causes low MW shift until single star-species are regenerated; however, no peaks at lower MWs were observed. The lack of molecular degradation was corroborated by DLS, as no decrease of the hydrodynamic volume was observed after dissociation of the aggregates. The aggregation was ascribed to changes in the solubility of MSW after the attachment of long polymeric chains, which also might induce a phase separation between hydrophobic core and polymer arms. A more detailed discussion of the process is given in the Supporting Information.

Synthesis and Characterization of $(PBiBEM_{300/450}\text{-}g\text{-}PnBA_{20/40/60/150})_6$ Star-Shaped Bottlebrushes. Due to the tendency of (**450-Br**)$_6$ to form aggregates, the solution of the polymer was sonicated prior to attempting the SCs grafting step, thus allowing for the restoration of individual macroinitiator species. Poly(*n*-butyl acrylate) (P*n*BA) side chains were grafted from (**450-Br**)$_6$ using the "grafting from" approach. Two polymerizations from the (**450-Br**)$_6$ were performed under normal ATRP conditions utilizing Cu^IBr/dNbpy catalysts with a ratio of [*n*BA]:[BiBEM] = [400]:[1]. The polymerizations were stopped at different monomer conversions, generating star-like bottlebrush polymers with DPs of P*n*BA grafts = 20 ((**450-*g*-20**)$_6$) and 40 ((**450-*g*-40**)$_6$). GPC analysis of (**450-*g*-20**)$_6$ and (**450-*g*-40**)$_6$ showed the shift of (**450-Br**)$_6$ peak signal toward higher MWs (Figure 2a, blue and green); however, some broadening of MWDs was also observed (Table 1, samples **3a** and **3b**). The higher M_w/M_n values of (**450-*g*-20**)$_6$ and (**450-*g*-40**)$_6$ were related to the presence of small fractions of high and/or low molecular weight shoulders in both GPC traces (Figure 2a, blue and green). The formation of high-molecular-weight (HMW) GPC peaks was likely due to small amounts of the residual macroinitiator aggregates that persisted during the side chains grafting as well as the possibility of the intermolecular coupling between growing macromolecules. On the other hand, the origin of the

Table 1. Characterization of Backbones and Star-like Bottlebrush Polymers Prepared from $MSW_{6\text{-}Br}$

				GPC		AFM	
sample	polymer structure	name/$DP_{arm\text{-}g\text{-}SC}$ [a]	$M_{n,th}$, $\times10^{-6}$ [b]	M_n, $\times10^{-6}$ [c]	M_w/M_n [c]	M_n, $\times10^{-6}$ [d]	M_w/M_n [e]
1	$[P(HEMA\text{-}TMS_{450})]_6$	(**450-TMS**)$_6$	0.55	0.27	1.22	N/A	N/A
2	$(PBiBEM_{450})_6$	(**450-Br**)$_6$	0.76	0.28[f]	1.39[f]	N/A	N/A
3a	$(PBiBEM_{450}\text{-}g\text{-}PnBA_{20})_6$	(**450-*g*-20**)$_6$	7.67	1.24	1.48	3.7	1.27
3b	$(PBiBEM_{450}\text{-}g\text{-}PnBA_{40})_6$	(**450-*g*-40**)$_6$	14.6	1.06	1.61	5.3	1.30
4	$[P(HEMA\text{-}TMS_{300})]_6$	(**300-TMS**)$_6$	0.37	0.16	1.12	N/A	N/A
5	$(PBiBEM_{300})_6$	(**300-Br**)$_6$	0.51	0.22	1.20	N/A	N/A
6a	$(PBiBEM_{300}\text{-}g\text{-}PnBA_{60})_6$	(**300-*g*-60**)$_6$	14.3	1.11	1.20	6.4	1.26
6b	$(PBiBEM_{300}\text{-}g\text{-}PnBA_{150})_6$	(**300-*g*-150**)$_6$	35.1	0.19	10.2	10.3	1.28

[a]Calculated from the monomer conversion obtained by ^1H NMR spectroscopy. $DP_{arm} = [A_{CH_2(polymer)}/A_{CH_2(monomer+polymer)}] \times [DP_{target}/6]$; where $A_{CH_2(monomer+polymer)}$ and $A_{CH_2(polymer)}$ are the respective areas under the curve corresponding to $-CH_2-$ protons of the polymer only and the monomer and the polymer total, and DP_{target} is a targeted DP of HEMA-TMS vs **$MSW_{6\text{-}Br}$**; $DP_{SC} = [1 - (A_{[nBA]}/A_{[nBA]_0})] \times DP_{target}$; where $A_{[nBA]}$ and $A_{[nBA]_0}$ are the integrations of vinyl protons of *n*BA vs anisole as an internal standard. [b]$M_{n,th} = 6 \times DP_{arm} \times (MW_{arm,monomer} + DP_{SCs} \times MW_{nBA}) + MW_{MSW}$. [c]Determined by THF GPC using linear PMMA standards. [d]Number-average molecular weight determined as a ratio of mass per unit area from LB film transfer and number of molecules per unit area from molecular imaging by AFM. [e]Molecular weight dispersity calculated by assuming a constant molecular weight per unit arm length for each sample. [f]Analyzed by DMF GPC using linear PMMA standards.

dx.doi.org/10.1021/ja506780y | J. Am. Chem. Soc. 2014, 136, 12762−12770

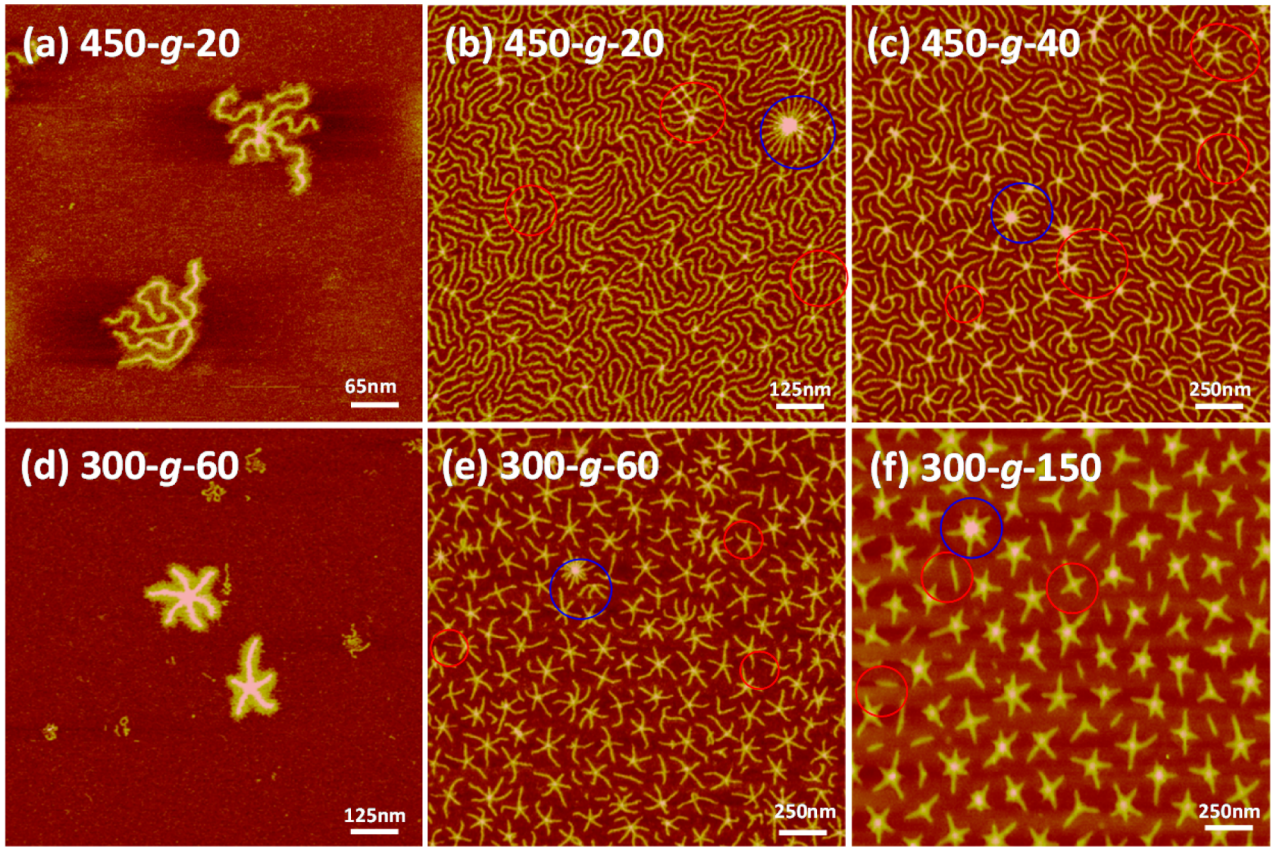

Figure 3. AFM height micrographs of (a) $(PBiBEM_{450}\text{-}g\text{-}PnBA_{20})_6$ ($(\mathbf{450\text{-}g\text{-}20})_6$), and (d) $(PBiBEM_{300}\text{-}g\text{-}PnBA_{60})_6$ ($(\mathbf{300\text{-}g\text{-}60})_6$) spin-cast from dilute chloroform solutions onto mica, and (b) $(PBiBEM_{450}\text{-}g\text{-}PnBA_{20})_6$ ($(\mathbf{450\text{-}g\text{-}20})_6$), (c) $(PBiBEM_{450}\text{-}g\text{-}PnBA_{40})_6$ ($(\mathbf{450\text{-}g\text{-}40})_6$), (e) $(PBiBEM_{300}\text{-}g\text{-}PnBA_{60})_6$ ($(\mathbf{300\text{-}g\text{-}60})_6$), and (f) $(PBiBEM_{300}\text{-}g\text{-}PnBA_{150})_6$ ($(\mathbf{300\text{-}g\text{-}150})_6$) prepared by Langmuir–Blodgett deposition using mica as the substrates. Blue circles indicate aggregated or/and cross-linked molecular stars, and red circles highlight structures with imperfections/missing arms/cross-links.

low-molecular-weight (LMW) peak was not fully understood. It has been tentatively ascribed to single arms, i.e., the linear bottlebrush. It was suspected that the highly congested structure of a star-shaped bottlebrush might be inducing a spontaneous cleavage of arms from the core. The loss of an arm would lead to relaxation of the highly strained architecture of the hexa-armed bottlebrush through the reduction of the steric hindrance between their bulky arms. GPC traces of $(\mathbf{450\text{-}g\text{-}20})_6$ and $(\mathbf{450\text{-}g\text{-}40})_6$ showed in both cases a presence of LMW polymers, which might indicate that the scission of arms from the highly congested core could occur in a solution for brush-stars arms with relatively short side chains.

In order to prepare a smaller star-shaped macroinitiator, shorter arms with DP = 300 ($(\mathbf{300\text{-}TMS})_6$) were polymerized from $\mathbf{MSW_{6\text{-}Br}}$. The reduction of the arm length should suppress the tendency of the polymer to form aggregates. The "grafting from" $(\mathbf{300\text{-}Br})_6$ was performed with a higher ratio of [*n*BA]:[BiBEM] = [1400]:[1], enabling longer side chains at lower monomer conversions and diminishing an intermolecular termination. Also, dNbpy was replaced with a more active ligand, PMDETA, to avoid a significant drop in the polymerization rate caused by dilution of the catalytic system. The reaction was stopped at 4.5% monomer conversion, giving P*n*BA molecular bottlebrush with average DP_{SC} = 60 of side chains ($(\mathbf{300\text{-}g\text{-}60})_6$). The GPC characterization showed a clear shift of $(\mathbf{300\text{-}Br})_6$ signal toward higher molecular weights (Figure 2b, blue), while keeping a low value of M_w/M_n = 1.20 (Table 1, sample **5**). Neither LMW nor HMW impurities were observed for $(\mathbf{300\text{-}g\text{-}60})_6$, which suggests that shorter arms (300 vs 450) result in less steric hindrance and provide enough space for the accommodation of brushes with longer side chains. The same polymerization conditions were used to graft longer side chains, reaching 11.1% monomer conversion and thus obtaining DP_{SC} = 150 of grafts ($(\mathbf{300\text{-}g\text{-}150})_6$). Interestingly, when compared to $(\mathbf{300\text{-}g\text{-}60})_6$, the star-brush with longer side chains displayed a much broader MWD, $M_w/M_n \approx 10$ (Table 1, sample **6b**) and a significant tailing toward LMWs in the GPC trace (Figure 2b, green). This indicated that noticeable degradation of the material occurred during the polymerization, suggesting that both grafts and the arm lengths contribute to the steric crowding in star-bottlebrushes, and most likely inducing scission of arms from the MSW core.

More accurate MWD data for star-shaped bottlebrushes were obtained by using a combination of molecular imaging by AFM and the Langmuir–Blodgett (LB) technique, which was shown to be particularly suitable for large branched macromolecules.[45]

AFM Characterization of Star-Shaped Bottlebrushes. AFM was employed to image both single molecules prepared by spin-casting and individual stars within dense monolayer prepared by the LB technique. The imaging process is greatly favored by spreading of the side chains, which increases both the persistence length of adsorbed bottlebrushes and the distance between the neighboring molecules.[5,33,61,62] Figure 3d,e depicts high-resolution images of single molecules that demonstrate distinct "octopus"- and "starfish"-like (with six or five arms) topologies for $(\mathbf{450\text{-}g\text{-}20})_6$ and $(\mathbf{300\text{-}g\text{-}60})_6$

dx.doi.org/10.1021/ja506780y | J. Am. Chem. Soc. 2014, 136, 12762–12770

respectively. AFM micrographs of LB monolayers of respective bottlebrushes $(\mathbf{450}\text{-}g\text{-}\mathbf{20})_6$, $(\mathbf{450}\text{-}g\text{-}\mathbf{40})_6$, $(\mathbf{300}\text{-}g\text{-}\mathbf{60})_6$, and $(\mathbf{300}\text{-}g\text{-}\mathbf{150})$ are depicted in Figure 3b,c,e,f. Similar to the single molecules, star-bottlebrushes exhibit a gradual change of the conformation from a worm-like shape to a rigid rod-like shape with increasing length of the grafts. This behavior is in agreement with literature reports on extension of the polymer backbone and the corresponding increase of the persistence length of bottlebrush macromolecules upon synthetic elongation of the side chains.[7,63]

High-resolution imaging of individual molecules by AFM was employed to characterize both MWD and length distribution of individual arms. Table 1 outlines the MWD data obtained by measuring mass per unit area from LB and number of molecules per unit area by AFM. The AFM-LB combination was shown to be particularly suitable for large branched macromolecules.[45] As expected, the AFM-LB numbers for M_n are higher than the corresponding numbers obtained by GPC that are usually underestimated for large and branched macromolecules. Clear resolution of the individual arms enabled accurate statistical analysis of the number arm length $\langle L_n \rangle$ as well as the arm length distribution $\langle L_w \rangle / \langle L_n \rangle$, as summarized in Table 2. The narrow length distributions ($\langle L_w \rangle /$ $\langle L_n \rangle \approx 1.1$) of arms in all star-like bottlebrushes proved the uniformity of structures, thus confirming well-controlled polymerization processes at each synthetic step (Table 2). In every case, arms in star-shaped bottlebrushes were extended, which was reflected in lengths of repeating units falling in the range of 0.23−0.25 nm. The values were close to the monomeric unit length in a fully extended zigzag chain (0.25 nm) and showed an excellent agreement of AFM results with the DPs of arms obtained from the monomer conversion by ^{1}H NMR spectroscopy (Table 2). However, the monomeric length of the arm in $(\mathbf{300}\text{-}g\text{-}\mathbf{150})_6$ was noticeably larger than 0.25 nm, which could be due to overestimation of the arm length in bottlebrushes with short arms and relatively long side chains.

Table 2. AFM Characterization of Star-Bottlebrushes

sample	name	$\langle L_n \rangle$ (nm)[a]	$\langle L_w \rangle / \langle L_n \rangle$[b]	$DP_{arm,NMR}$	$\langle L_{mon} \rangle$ (nm)[c]
3a	$(\mathbf{450}\text{-}g\text{-}\mathbf{20})_6$	105 ± 3	1.09	450	0.23 ± 0.01
3b	$(\mathbf{450}\text{-}g\text{-}\mathbf{40})_6$	112 ± 3	1.07	450	0.25 ± 0.01
6a	$(\mathbf{300}\text{-}g\text{-}\mathbf{60})_6$	69 ± 2	1.09	300	0.23 ± 0.01
6b	$(\mathbf{300}\text{-}g\text{-}\mathbf{150})_6$	95 ± 2	1.12	300	0.32 ± 0.01

[a]Number-average contour length of the individual arms of star-like bottlebrushes imaged by AFM. [b]Length dispersity: the ratio of weight-average ($\langle L_w \rangle$) and number-average ($\langle L_n \rangle$) arm lengths, determined as $\langle L_w \rangle / \langle L_n \rangle = \langle L_n^2 \rangle / \langle L_n \rangle^2$. [c]$\langle L_{mon} \rangle = \langle L_n \rangle / DP_{arm,NMR}$.

AFM images also allowed clear visualization of several types of structural imperfections in the obtained star-shaped bottlebrushes (Figure 3). First, we observed single molecules with more than six arms (blue circles), which could be ascribed to physical aggregation of $(\mathbf{450}\text{-}\mathbf{Br})_6$ macroinitiators during the side chain grafting. Second, a few irregular structures with interconnected arms linking several star-like brushes were also noticed (blue circles). This was attributed to the coupling between growing arms of P(HEMA-TMS) stars ($(\mathbf{450}\text{-}\mathbf{TMS})_6$ and $(\mathbf{300}\text{-}\mathbf{TMS})_6$) during ATRP processes. Third, a significant fraction of macromolecules with the number of arms lower than six (red circles) was observed which might have two origins: (i) synthetic and (ii) physical. The less than 6 number of arms could be related to the limited initiation efficiency from $\mathbf{MSW}_{6\text{-}\mathbf{Br}}$ initiator as reported previously for the fabrication of three- and four-armed brush polymers.[33] The second cause is mechanical cleavage of the arms due to the strong tension enhancement at the branching core of the bottlebrush stars.

As reported previously, bottlebrush structures are able to generate significant tension in their backbone due to steric repulsion between densely grafted side chains.[64] Depending on the side-chain length and grafting density, and the interaction with the surrounding environment (solvent, substrate, neighboring macromolecules), the backbone tension can be amplified from the pico-Newton to nano-Newton range. Mechanical forces of this magnitude are sufficient to break covalent bonds.[7,65] Additional amplification of bond tension occurs in tethered bottlebrushes that also exhibit a gradient of tension due to steric repulsion between the neighboring bottlebrushes.[66] As shown in Figure 4, for the star-brush $(\mathbf{300}\text{-}g\text{-}\mathbf{150})_6$, after adsorption on water/2-propanol (99.5/0.5 wt/wt %) mica surface for 3 h, the number fraction of molecules with one and two arms increased from ∼25% to 35%, accompanied by the corresponding decrease in the number fractions of molecules with three, four, five, and six arms, while the average length of arms hardly changed. This indicates that bottlebrush stars undergo preferential cleavage of the arms from the MSW core. After 24 h, there were almost no molecules with multiple arms remained. In addition, the average arm length decreased by ∼20 nm, suggesting scission of covalent bonds in the backbone of individual bottlebrush arms, which occurred at a slower rate than the arm cleavage process.

The preferential cleavage of the arms was ascribed to stronger steric repulsion of neighboring arms at the MSW core (Figure 4f). In addition, the ester bond connecting the core and the arm could be more vulnerable than C−C bonds under aqueous conditions,[64] which might also favor the cleavage of the arms. In contrast, neither the cleavage of the arms nor the backbone scission within the arms was observed for the star-brushes with shorter side chains within 24 h, i.e., $(\mathbf{450}\text{-}g\text{-}\mathbf{20})_6$, $(\mathbf{450}\text{-}g\text{-}\mathbf{40})_6$ and $(\mathbf{300}\text{-}g\text{-}\mathbf{60})_6$ (Figure S11). This was due to the short grafts that were not able to generate large enough tension along the backbone to break a covalent bond.

SUMMARY

In conclusion, a rational design of a rigid, well-defined molecular spoked wheel hexa-ATRP initiator allowed for the preparation of polymeric materials with novel properties, allowing for focusing tension to specific bonds and potentially selective bond activation/scission. Star-shaped bottlebrushes were synthesized via the combination of advanced synthetic methods and ATRP. Side chains were grafted from star-shaped macroinitiators yielding the following polymers: $(\mathbf{450}\text{-}g\text{-}\mathbf{20})_6$, $(\mathbf{450}\text{-}g\text{-}\mathbf{40})_6$, $(\mathbf{300}\text{-}g\text{-}\mathbf{60})_6$ and $(\mathbf{300}\text{-}g\text{-}\mathbf{150})_6$. AFM imaging of such architectures confirmed the unusual "starfish"- and "octopus"-like topologies of star-brush polymers, proving the successful synthesis of these complex polymeric architectures. During the synthesis, it was discovered that PBiBEM macroinitiators $(\mathbf{450}\text{-}\mathbf{Br})_6$ demonstrate a strong tendency to form physical aggregates through the hydrophobic interactions of MSW cores. The association process was prevented by sonication of polymer solutions prior to the analysis and brush synthesis. Reported star-like brush polymers represent a new class of polymers that integrate the properties of both bottlebrushes and MSWs. The cleavage of the arms from the MSW core occurred preferentially, which may shed light on the

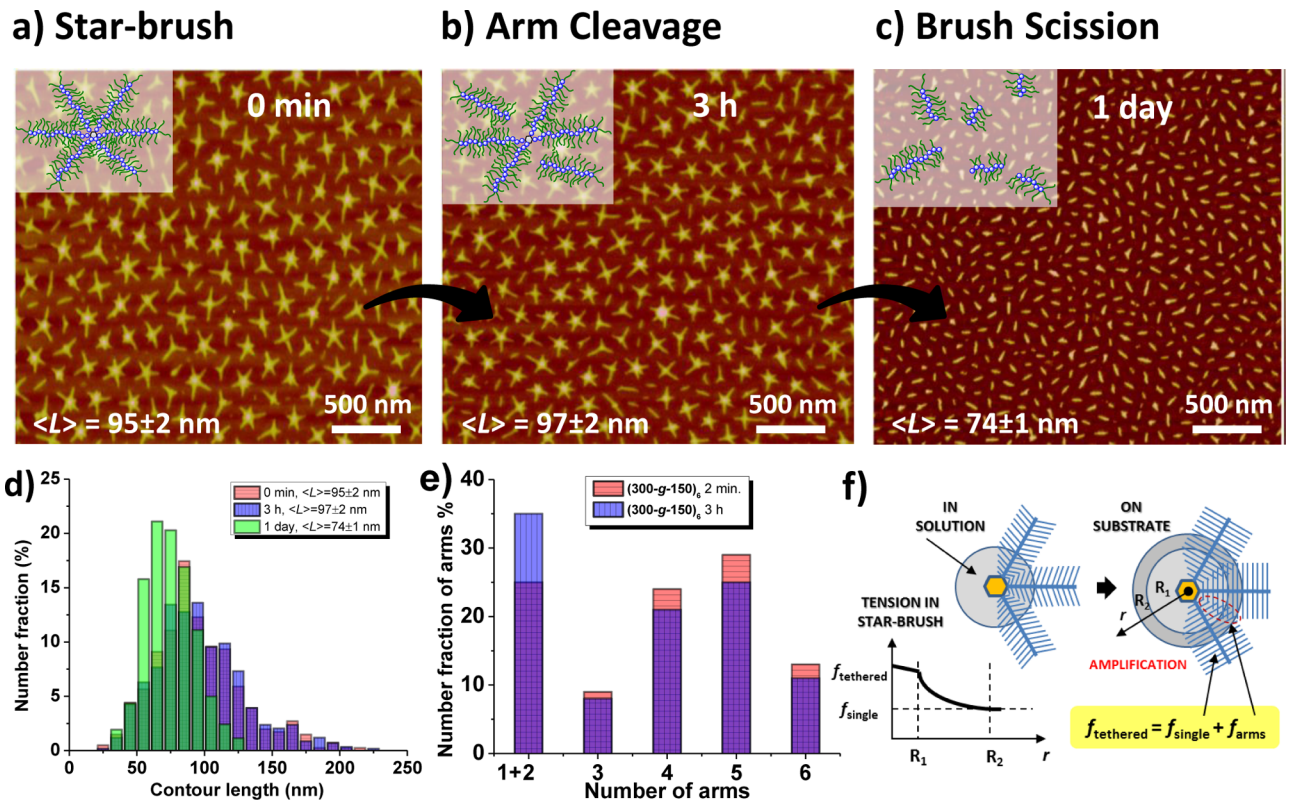

Figure 4. AFM height micrographs of LB films of $(300\text{-}g\text{-}150)_6$ transferred from water/2-propanol (99.5/0.5 wt/wt %) surface onto mica substrates after (a) 2 min, (b) 3 h, and (c) 1 day. (d) The number distribution of contour length of $(300\text{-}g\text{-}150)_6$ after 2 min (red), 3 h (blue), and 1 day (green) (more than 400 molecules counted). (e) The number fraction of objects with different numbers of arms. (f) A schematic representation of the side chains tapering near the core in solution and the amplification of force on the substrate.

design of molecular tensile machines that can focus mechanical tension on specific bonds.

EXPERIMENTAL SECTION

The following describes the synthesis and characterization of polymers.

Materials. *n*-Butyl acrylate (*n*BA, 99%, Acros) and (2-trimethylsiloxy)ethyl methacrylate (HEMA-TMS, Scientific Polymer Products) were purified by passing the monomer through a column filled with basic alumina to remove the inhibitor. All other reagents: copper(I) bromide (Cu^IBr, 99.999%), copper(II) bromide ($Cu^{II}Br_2$, 99.999%), copper(I) chloride (Cu^ICl, 99.995%), copper(II) chloride ($Cu^{II}Cl_2$, 99.999%), 4,4′-dinonyl-2,2′-dipyridyl (dNbpy, 97%) *N,N,N′,N″,N″*-pentamethyldiethylenetriamine (PMDETA, 99%), potassium fluoride (KF, 99%), tetrabutylammonium fluoride (TBAF, 1.0 M in THF), α-bromoisobutyryl bromide (98%), 2,5-di-*tert*-butylphenol (DTBP, 99%), triethylamine (TEA, ≤99%), and solvents were purchased from Aldrich and used as received without further purification.

Characterization. The conversion of *n*BA was determined from ^{1}H NMR spectra recorded in $CDCl_3$ as a solvent using Brüker 300 MHz spectrometer. The particle size was measured using a Zetasizer Nano from Malvern Instruments. The sonication was performed using Ultrasonic cleaner model FS20 from Fisher Scientific with a sweep frequency of 40 kHz. MWDs of the polymers were characterized by GPC using Polymer Standards Services columns (guard, 10^5, 10^3, and 10^2 Å), with THF eluent at 35 °C, flow rate 1.00 mL/min, and differential refractive index detector (Waters, 2410). The apparent number-average molecular weights (M_n) and molecular weight dispersities (M_w/M_n) were determined with a calibration based on linear PMMA standards and diphenyl ether as an internal standard, using WinGPC 6.0 software from Polymer Standards Services. In addition, the M_n was measured by the AFM-LB method described elsewhere.[67] The samples for AFM measurement were prepared by either LB deposition or spin-casting from dilute solutions. LB films were transferred onto freshly cleaved mica substrates at a constant surface pressure of 0.5 mN/m and a controlled transfer ratio. Imaging of individual molecules was performed in PeakForce QNM mode using a multimode AFM (Brüker) with a NanoScope V controller. We used silicon probes with a resonance frequency of 50−90 Hz and a spring constant of ∼0.4 N/m. In-house developed computer software was used to analyze the AFM images with respect to arm size and MWD of star-like bottlebrushes. Typically, ensembles of 200−300 molecules were analyzed to ensure standard deviation of the mean below 10%.

Synthesis of 1, $[P(HEMA\text{-}TMS)_{450}]_6$ $(450\text{-}TMS)_6$. A 10 mL Schlenk flask was charged with $\mathbf{MSW}_{6\text{-}Br}$ (0.0137 g, 0.0019 mmol), HEMA-TMS (4.0 mL, 18.4 mmol), dNbpy (0.023 g, 0.056 mmol), $Cu^{II}Cl_2$ (0.62 mg, 0.0046 mmol), and anisole (1.0 mL). The solution was degassed by three freeze−pump−thaw cycles. During the final cycle, the flask was filled with nitrogen, and Cu^ICl (22.6 mg, 0.0230 mmol) was quickly added to the frozen reaction mixture. The flask was sealed, evacuated and back-filled with nitrogen five times, and then immersed in an oil bath at 60 °C. Polymerization was terminated after 69 h reaching 26.1% conversion as determined by ^{1}H NMR, which corresponded to DP ≈ 450 per arm. Apparent molecular weight determined by THF GPC: $M_{n,GPC} = 2.70 \times 10^5$, and $M_w/M_n = 1.22$. The reaction mixture was diluted with chloroform, passed through neutral alumina to remove the catalyst, then concentrated and used for the next step without further purification.

Synthesis of 2, $(PBiBEM_{450})_6$ $(450\text{-}Br)_6$. A 50 mL round-bottom flask was charged with **1** (1.711 g, 5.80 mmol), KF (0.513 g, 8.70 mmol), DTBP (0.120 g, 0.580 mmol), and then dry THF (15 mL) was added under nitrogen. The reaction mixture was cooled down in an ice bath, followed by the injection of TBAF (0.12 mL, 1.0 M in THF, 0.120 mmol) and subsequent dropwise addition of α-bromoisobutyryl bromide (2.67 g, 1.43 mL. 11.6 mmol) over the

dx.doi.org/10.1021/ja506780y | J. Am. Chem. Soc. 2014, 136, 12762−12770

course of 10 min. Upon addition, the reaction mixture was allowed to reach room temperature and was stirred for another 16 h. Afterward solids were filtered off and the mixture was precipitated into methanol/water (70/30), re-dissolved in chloroform (30 mL), and passed through the column filled with basic alumina. The product **2** was re-precipitated three times in hexanes and dried overnight under vacuum. Apparent molecular weight determined by THF GPC: $M_{n,GPC}$ = 2.80 × 10^5, and M_w/M_n = 1.39.

Synthesis of 3a, (PBiBEM$_{450}$-*g*-P*n*BA$_{20}$)$_6$ (450-*g*-20)$_6$. A 25 mL Schlenk flask equipped with a stir bar was charged with macroinitiator **2** (0.0870 g, 0.3086 mmol of BiBEM groups), *n*BA (17.6 mL, 123.4 mmol), dNbpy (0.126 g, 0.309 mmol), $Cu^{II}Br_2$ (1.7 mg, 0.0077 mmol), and anisole (2.5 mL). The solution was degassed by three freeze−pump−thaw cycles. During the final cycle $Cu^{I}Br$ (21.0 mg, 0.1466 mmol) was quickly added to the frozen reaction mixture under nitrogen atmosphere. The flask was sealed, evacuated and back-filled with nitrogen five times, and then immersed in an oil bath thermostated at 60 °C. The polymerization was stopped after 20 h, and the monomer conversion was determined by both gravimetry and ^{1}H NMR, resulting in the brush polymer **3a** with DP ≈ 20 of side chains. The polymer was purified by three precipitations from cold methanol, and dried under vacuum at room temperature, to a constant mass. Apparent molecular weight was determined using THF GPC: $M_{n,GPC}$ = 1.24 × 10^6, and M_w/M_n = 1.48.

Synthesis of 3b, (PBiBEM$_{450}$-*g*-P*n*BA$_{40}$)$_6$ (450-*g*-40)$_6$. The reaction was set up and analyzed in the same way as **3a** except the reaction temperature was 70 °C. The amounts of reagents used for the polymerization: macroinitiator **2** (0.0554 g, 0.1964 mmol of BiBEM groups), *n*BA (11.2 mL, 78.6 mmol), dNbpy (0.080 g, 0.196 mmol), $Cu^{II}Br_2$ (1.1 mg, 0.0049 mmol), anisole (1.25 mL) and $Cu^{I}Br$ (13.3 mg, 0.0933 mmol). The polymerization was stopped after 23 h 20 min, giving the brush polymer, **3b**, with DP = 40 of side chains. Apparent molecular weight determined by THF GPC: $M_{n,GPC}$ = 1.06 × 10^6, and M_w/M_n = 1.61.

Synthesis of 4, [P(HEMA-TMS)$_{300}$]$_6$ (300-TMS)$_6$. The reaction was set up and analyzed in the same way as **1**. The amounts of reagents used for the polymerization: **MSW$_{6\text{-Br}}$** ATRP initiator (0.0164 g, 0.0023 mmol), HEMA-TMS (3.0 mL, 17.2 mmol), dNbpy (0.017 g, 0.041 mmol), $Cu^{II}Cl_2$ (0.46 mg, 0.0034 mmol), anisole (0.75 mL), and $Cu^{I}Cl$ (1.7 mg, 0.0172 mmol). The polymerization was stopped after 39 h 10 min reaching 30.1% conversion, giving the polymer, **4**, with DP ≈ 300 per arm. Apparent molecular weight determined by THF GPC: $M_{n,GPC}$ = 1.64 × 10^5, and M_w/M_n = 1.12.

Synthesis of 5, (PBiBEM$_{300}$)$_6$ (300-Br)$_6$. The reaction was set up and analyzed in the same way as **2**. The amounts of reagents used for the functionalization: the polymer **4** (0.50 g, 2.5 mmol), KF (0.161 g, 2.72 mmol), DTBP (0.051 g, 0.248 mmol), dry THF (15 mL), TBAF (0.013 mL, 1.0 M in THF, 0. 013 mmol), and α-bromoisobutyryl bromide (0.626 g, 0.37 mL, 2.72 mmol) over the course of 10 min. The reaction was performed twice to ensure quantitative functionalization of the macroinitiator **5**. The polymer was purified by dialysis against THF using 50 kDa MWCO membranes. The polymer was stored as a solution in anisole to avoid aggregation. Apparent molecular weight determined by THF GPC: $M_{n,GPC}$ = 2.23 × 10^5, and M_w/M_n = 1.20.

Synthesis of 6a, (PBiBEM$_{300}$-*g*-P*n*BA$_{60}$)$_6$ (300-*g*-60)$_6$. The reaction was set up and analyzed in the same way as **3a**. The amounts of reagents used for the polymerization: macroinitiator **5** (0.0283 g, 0.0993 mmol of BiBEM groups), *n*BA (19.8 mL, 139.0 mmol), PMDETA (0.0086g, 10.4 μL, 0.0496 mmol), $Cu^{II}Br_2$ (0.55 mg, 0.0025 mmol), anisole (2.2 mL), and $Cu^{I}Br$ (6.7 mg, 0.0472 mmol). The polymerization was stopped after 15 h 30 min, giving the brush polymer, **6a**, with DP = 60 of side chains. Apparent molecular weight determined by THF GPC: $M_{n,GPC}$ = 1.11 × 10^6, and M_w/M_n = 1.20.

Synthesis of 6b, (PBiBEM$_{300}$-*g*-P*n*BA$_{150}$)$_6$ (300-*g*-150)$_6$. The reaction was set up and analyzed in the same way as **6a**. The polymerization was stopped after 49 h 30 min, giving the brush polymer, **6b**, with DP = 150 of side chains. Apparent molecular weight determined by THF GPC: $M_{n,GPC}$ = 1.93 × 10^5, and M_w/M_n = 10.2.

■ ASSOCIATED CONTENT

Supporting Information

Detailed synthesis and characterization of the initiator, **MSW$_{6\text{-Br}}$**, and all its precursors; discussion and characterization of the aggregation of **(450-Br)$_6$**; and distribution of number of arms in star-shaped objects. This material is available free of charge via the Internet at http://pubs.acs.org.

■ AUTHOR INFORMATION

Corresponding Authors

hoeger@uni-bonn.de
sergei@email.unc.edu
km3b@andrew.cmu.edu

Notes

The authors declare no competing financial interest.

■ ACKNOWLEDGMENTS

Support from the National Science Foundation (DMR-0969301 and DMR-1122483), the DFG (SFB 624), and the Fonds der Chemischen Industrie is acknowledged.

■ REFERENCES

(1) Webster, O. W. *Science* **1991**, *251*, 887.
(2) Hawker, C. J.; Wooley, K. L. *Science* **2005**, *309*, 1200.
(3) Braunecker, W. A.; Matyjaszewski, K. *Prog. Polym. Sci.* **2007**, *32*, 93.
(4) Beers, K. L.; Gaynor, S. G.; Matyjaszewski, K.; Sheiko, S. S.; Moeller, M. *Macromolecules* **1998**, *31*, 9413.
(5) Sheiko, S. S.; Prokhorova, S. A.; Beers, K. L.; Matyjaszewski, K.; Potemkin, I. I.; Khokhlov, A. R.; Moeller, M. *Macromolecules* **2001**, *34*, 8354.
(6) Zhang, M.; Mueller, A. H. E. *J. Polym. Sci., Part A: Polym. Chem.* **2005**, *43*, 3461.
(7) Sheiko, S. S.; Sun, F. C.; Randall, A.; Shirvanyants, D.; Rubinstein, M.; Lee, H.-i.; Matyjaszewski, K. *Nature* **2006**, *440*, 191.
(8) Sheiko, S. S.; Sumerlin, B. S.; Matyjaszewski, K. *Prog. Polym. Sci.* **2008**, *33*, 759.
(9) Gao, H.; Matyjaszewski, K. *Prog. Polym. Sci.* **2009**, *34*, 317.
(10) Lee, H.-i.; Pietrasik, J.; Sheiko, S. S.; Matyjaszewski, K. *Prog. Polym. Sci.* **2010**, *35*, 24.
(11) Tang, C.; Dufour, B.; Kowalewski, T.; Matyjaszewski, K. *Macromolecules* **2007**, *40*, 6199.
(12) Lecommandoux, S.; Chécot, F.; Borsali, R.; Schappacher, M.; Deffieux, A.; Brulet, A.; Cotton, J. P. *Macromolecules* **2002**, *35*, 8878.
(13) Neugebauer, D.; Zhang, Y.; Pakula, T.; Matyjaszewski, K. *Macromolecules* **2005**, *38*, 8687.
(14) Gao, H.; Matyjaszewski, K. *J. Am. Chem. Soc.* **2007**, *129*, 6633.
(15) Cheng, G.; Boeker, A.; Zhang, M.; Krausch, G.; Mueller, A. H. E. *Macromolecules* **2001**, *34*, 6883.
(16) Boerner, H. G.; Beers, K.; Matyjaszewski, K.; Sheiko, S. S.; Moeller, M. *Macromolecules* **2001**, *34*, 4375.
(17) Sumerlin, B. S.; Neugebauer, D.; Matyjaszewski, K. *Macromolecules* **2005**, *38*, 702.
(18) Matyjaszewski, K.; Tsarevsky, N. V. *J. Am. Chem. Soc.* **2014**, *136*, 6513.
(19) Matyjaszewski, K.; Xia, J. *Chem. Rev.* **2001**, *101*, 2921.
(20) Matyjaszewski, K.; Tsarevsky, N. V. *Nat. Chem.* **2009**, *1*, 276.
(21) Huang, K.; Rzayev, J. *J. Am. Chem. Soc.* **2009**, *131*, 6880.
(22) Li, Z.; Zhang, K.; Ma, J.; Cheng, C.; Wooley, K. L. *J. Polym. Sci., Part A: Polym. Chem.* **2009**, *47*, 5557.
(23) Zehm, D.; Laschewsky, A.; Liang, H.; Rabe, J. P. *Macromolecules* **2011**, *44*, 9635.
(24) Stals, P. J. M.; Li, Y.; Burdyńska, J.; Nicolaÿ, R.; Nese, A.; Palmans, A. R. A.; Meijer, E. W.; Matyjaszewski, K.; Sheiko, S. S. *J. Am. Chem. Soc.* **2013**, *135*, 11421.

(25) Lee, H.-i.; Jakubowski, W.; Matyjaszewski, K.; Yu, S.; Sheiko, S. S. *Macromolecules* **2006**, *39*, 4983.
(26) Rzayev, J. *Macromolecules* **2009**, *42*, 2135.
(27) Bolton, J.; Bailey, T. S.; Rzayev, J. *Nano Lett.* **2011**, *11*, 998.
(28) Miyake, G. M.; Piunova, V. A.; Weitekamp, R. A.; Grubbs, R. H. *Angew. Chem., Int. Ed.* **2012**, *51*, 11246.
(29) Sveinbjörnsson, B. R.; Weitekamp, R. A.; Miyake, G. M.; Xia, Y.; Atwater, H. A.; Grubbs, R. H. *Proc. Natl. Acad. Sci. U.S.A.* **2012**, *109*, 14332.
(30) Yu-Su, S. Y.; Sheiko, S. S.; Lee, H.-i.; Jakubowski, W.; Nese, A.; Matyjaszewski, K.; Anokhin, D.; Ivanov, D. A. *Macromolecules* **2009**, *42*, 9008.
(31) Lee, H.-i.; Matyjaszewski, K.; Yu, S.; Sheiko, S. S. *Macromolecules* **2005**, *38*, 8264.
(32) Elsen, A. M.; Li, Y.; Li, Q.; Sheiko, S. S.; Matyjaszewski, K. *Macromol. Rapid Commun.* **2014**, *35*, 133.
(33) Matyjaszewski, K.; Qin, S.; Boyce, J. R.; Shirvanyants, D.; Sheiko, S. S. *Macromolecules* **2003**, *36*, 1843.
(34) Zhang, Y.; Constantini, N.; Mierzwa, M.; Pakula, T.; Neugebauer, D.; Matyjaszewski, K. *Polymer* **2004**, *45*, 6333.
(35) Pakula, T.; Zhang, Y.; Matyjaszewski, K.; Lee, H.-i.; Boerner, H.; Qin, S.; Berry, G. C. *Polymer* **2006**, *47*, 7198.
(36) Miyake, G. M.; Weitekamp, R. A.; Piunova, V. A.; Grubbs, R. H. *J. Am. Chem. Soc.* **2012**, *134*, 14249.
(37) Chen, P.; Li, C.; Liu, D.; Li, Z. *Macromolecules* **2012**, *45*, 9579.
(38) Ding, J.; Xiao, C.; Tang, Z.; Zhuang, X.; Chen, X. *Macromol. Biosci.* **2011**, *11*, 192.
(39) Ding, J.; Xiao, C.; Zhao, L.; Cheng, Y.; Ma, L.; Tang, Z.; Zhuang, X.; Chen, X. *J. Polym. Sci., Part A: Polym. Chem.* **2012**, *49*, 2665.
(40) Wu, D.; Nese, A.; Pietrasik, J.; Yeru Liang, M. K.; Huang, L.; Kowalewski, T.; Matyjaszewski, K. *ACS Nano* **2012**, *6*, 6208.
(41) Sun, G.; Cho, S.; Clark, C.; Verkhoturov, S. V.; Eller, M. J.; Li, A.; Pavía-Jiménez, A.; Schweikert, E. A.; Thackeray, J. W.; Trefonas, P.; Wooley, K. L. *J. Am. Chem. Soc.* **2013**, *135*, 4203.
(42) Hong, S. W.; Gu, W.; Huh, J.; Sveinbjornsson, B. R.; Jeong, G.; Grubbs, R. H.; Russell, T. P. *ACS Nano* **2013**, *7*, 9684.
(43) Boyce, J. R.; Shirvanyants, D.; Sheiko, S. S.; Ivanov, D. A.; Qin, S.; Börner, H.; Matyjaszewski, K. *Langmuir* **2004**, *20*, 6005.
(44) Iyoda, M.; Yamakawa, J.; Rahman, M. J. *Angew. Chem., Int. Ed.* **2011**, *50*, 10522.
(45) Höger, S. *Pure Appl. Chem.* **2010**, *82*, 821.
(46) Haley, M. *Pure Appl. Chem.* **2008**, *80*, 519.
(47) Zhang, W.; Moore, J. S. *Angew. Chem., Int. Ed.* **2006**, *45*, 4416.
(48) Bunz, U. H. F.; Rubin, Y.; Tobe, Y. *Chem. Soc. Rev.* **1999**, *28*, 107.
(49) Mössinger, D.; Hornung, J.; Lei, S.; De Feyter, S.; Höger, S. *Angew. Chem., Int. Ed.* **2007**, *46*, 6802.
(50) Aggarwal, V.; Thiessen, A.; Idelson, A.; Kalle, D.; Würsch, D.; Stangl, T.; Steiner, F.; Jester, S.-S.; Vogelsang, J.; Höger, S.; Lupton, J. M. *Nat. Chem.* **2013**, *5*, 964.
(51) Mössinger, D.; Chaudhuri, D.; Kudernac, T.; Lei, S.; De Feyter, S.; Lupton, J. M.; Höger, S. *J. Am. Chem. Soc.* **2010**, *132*, 1410.
(52) Lei, S.; Ver Heyen, A.; De Feyter, S.; Surin, M.; Lazzaroni, R.; Rosenfeldt, S.; Ballauff, M.; Lindner, P.; Mössinger, D.; Höger, S. *Chem.—Eur. J.* **2009**, *15*, 2518.
(53) Höger, S.; Tahara, K.; Lei, S.; Mössinger, D.; Kozuma, H.; Inukai, K.; Van der Auweraer, M.; De Schryver, F. C.; Tobe, Y.; De Feyter, S. *Chem. Commun.* **2008**, 3897.
(54) Schwartz, B. J. *Nat. Mater.* **2008**, *7*, 427.
(55) Schwartz, B. J. *Annu. Rev. Phys. Chem.* **2003**, *54*, 141.
(56) Dawn, S.; Dewal, M. B.; Sobransingh, D.; Paderes, M. C.; Wibowo, A. C.; Smith, M. D.; Krause, J. A.; Pellechia, P. J.; Shimizu, L. S. *J. Am. Chem. Soc.* **2011**, *133*, 7025.
(57) Li, Y.; Nese, A.; Hu, X.; Lebedeva, N. V.; LaJoie, T. W.; Burdyńska, J.; Stefan, M. C.; You, W.; Yang, W.; Matyjaszewski, K.; Sheiko, S. S. *ACS Macro Lett.* **2014**, *3*, 738.
(58) Aggarwal, A. V.; Jester, S.-S.; Taheri, S. M.; Förster, S.; Höger, S. *Chem.—Eur. J.* **2013**, *19*, 4480.
(59) Matyjaszewski, K.; Shipp, D. A.; Wang, J.-L.; Grimaud, T.; Patten, T. E. *Macromolecules* **1998**, *31*, 6836.
(60) Neugebauer, D.; Zhang, Y.; Pakula, T.; Sheiko, S. S.; Matyjaszewski, K. *Macromolecules* **2003**, *36*, 6746.
(61) Borner, H. G.; Duran, D.; Matyjaszewski, K.; da Silva, M.; Sheiko, S. S. *Macromolecules* **2002**, *35*, 3387.
(62) Pietrasik, J.; Sumerlin, B. S.; Lee, H.-i.; Gil, R. R.; Matyjaszewski, K. *Polymer* **2007**, *48*, 496.
(63) Elli, S.; Ganazzoli, F.; Timoshenko, E. G.; Kuznetsov, Y. A.; Connolly, R. *J. Chem. Phys.* **2004**, *120*, 6257.
(64) Schmidt, S. W.; Kersch, A.; Beyer, M. K.; Clausen-Schaumann, H. *Phys. Chem. Chem. Phys.* **2011**, *13*, 5994.
(65) Lebedeva, N. V.; Nese, A.; Sun, F. C.; Matyjaszewski, K.; Sheiko, S. S. *Proc. Natl. Acad. Sci. U.S.A.* **2012**, *109*, 9276.
(66) Sheiko, S. S.; Panyukov, S.; Rubinstein, M. *Macromolecules* **2011**, *44*, 4520.
(67) Sheiko, S. S.; da Silva, M.; Shirvaniants, D. G.; LaRue, I.; Prokhorova, S. A.; Moeller, M.; Beers, K.; Matyjaszewski, K. *J. Am. Chem. Soc.* **2003**, *125*, 6725.